AEM
Journals.ASM.org

Homologous Alkalophilic and Acidophilic L-Arabinose Isomerases Reveal Region-Specific Contributions to the pH Dependence of Activity and Stability

Sang-Jae Lee,[a] Sang Jun Lee,[b] Yong-Jik Lee,[b] Seong-Bo Kim,[c] Sung-Kun Kim,[d] and Dong-Woo Lee[a]

Division of Applied Biology and Chemistry, Kyungpook National University, Daegu, South Korea[a]; Systems and Synthetic Biology Research Center, Korea Research Institute of Bioscience and Biotechnology, Daejeon, South Korea[b]; CJ Foods R & D, CJ Cheiljedang Corporation, Seoul, South Korea[c]; and Department of Chemistry and Biochemistry, Baylor University, Waco, Texas, USA[d]

To study the pH dependence of L-arabinose isomerase (AI) activity and stability, we compared homologous AIs with their chimeras. This study demonstrated that an ionizable amino acid near the catalytic site determines the optimal pH (pH_{opt}) for activity, whereas the N-terminal surface R residues play an important role in determining the pH_{opt} for stability.

Unlike neutrophilic enzymes, many proteins expressed by acidophiles and alkalophiles exhibit maximal activities beyond neutral pH conditions (3, 5, 12, 19, 25). It has been noted that the optimum pH (pH_{opt}) of the maximal catalytic rate of an enzyme is primarily affected by the pK_a values of ionizable groups on the catalytic and substrate binding sites (1, 19, 28, 29). On the other hand, the pH_{opt} for maximal protein stability, defined as the pH at which the free energy of unfolding (ΔG_U) is lowest, is likely to be dependent on the base/acid ratio of surface groups (27) and the net charge of each specific structural region (6, 24). A numerical approach (1) demonstrated that pH stability is not directly related to the isoelectric point (pI) of a protein (4). Denaturation experiments also suggested that the pH dependence of the thermodynamic stability (ΔG_U) of a protein arises as a consequence of differential pK_a values attained in the folded and unfolded states (2, 27).

Thermostable L-arabinose isomerases (AI; EC 5.3.1.4) are utilized for the production of D-tagatose as a sugar replacement (13, 15, 18, 22). To achieve high yields of D-tagatose production, isomerization at high temperatures (~60°C) and acidic pH (≤6.0) is considered the most favorable condition for minimizing unwanted byproduct formation and browning effects (8, 19). Hence, for the rational design and engineering of a thermoacidophilic AI, the relationships between sequence, structure, and function with respect to the pH dependence of AIs must be better understood. Therefore, we characterized the thermoalkalophilic AI from a newly isolated *Alicyclobacillus* sp. TP7 strain in comparison with its acidic counterpart (19). Although the two AIs showed >82% amino acid sequence similarity, their pH_{opt} values differ by 3 to 3.5 U. To better understand the molecular basis of differences in the pH dependence of their activity and stability, we generated AI chimeras by homologous recombination and site-directed mutagenesis and characterized them.

Isolation of the *araA* gene and characterization of AI. To isolate thermoacidophiles producing AIs, over 200 samples from hot springs in Indonesia were cultured on EM-1 medium (16) supplemented with L-arabinose at pH 2 and 65°C (see the supplemental material). From these, 20 strains were isolated and assayed for AI activity as described in reference 10. Isolate TP7, which showed the highest AI activity, was selected and its 16S rRNA gene sequence was determined (30). Sequencing revealed a 97% to 99% similarity with *Alicyclobacillus* strains (see Fig. S1 in the supplemental material). Therefore, isolate TP7 was identified as *Alicyclobacillus* sp. TP7 (Korean Collection for Type Cultures 33088). To obtain the *araA* gene encoding AI, the degenerate primers DaraAF and DaraAR were designed based on the internal amino acid sequences of *araA* genes (see the supplemental material) (19). The intact *araA* gene of *Alicyclobacillus* sp. TP7 (GenBank accession number JQ945232) was amplified by PCR, and the resulting DNA was cloned into the pET 22b(+) vector to generate pET-ASAI. Sequence analysis demonstrated that the 1,485-bp *araA* gene encoded a 494-amino-acid polypeptide (*Alicyclobacillus* sp. TP7 AI [ASAI]). The presumed ASAI amino acid sequence showed high (68% to 96%) similarity to those of other AIs from *A. acidocaldarius* (7, 19, 21) and *Geobacillus stearothermophilus* (17).

The characterization of purified ASAI is summarized in Table S1 in the supplemental material. The relative molecular weight (M_r) of ASAI was estimated to be 56 based on SDS-PAGE. However, native PAGE and gel filtration chromatography suggested that the native form of ASAI exists as a homotetramer (M_r = ~220). The pH_{opt} of ASAI activity was 8.5 at 70°C, and ASAI retained its original activity (>95%) even after 20 h of incubation at pH 7 to 9. The K_m and V_{max} of ASAI for L-arabinose were determined to be 49.7 mM and 52.4 μmol/mg · min at pH 8.5 (70°C). ASAI was activated by the addition of 1 mM Mn^{2+} (2.0-fold) and 1 mM Mg^{2+} (1.5-fold), whereas 1 mM EDTA inhibited AI activity (17–19).

Generation of functional AI chimeras. The crystal structure of *Escherichia coli* L-arabinose isomerase (ECAI) (20), together with the results of our previous work (14, 19), suggested that the N- and C-terminal domains of AIs might contribute to the physicochemical properties of activity and stability, respectively. In addition, K269 in *Alicyclobacillus acidocaldarius* AI (AAAI) was found to play an important role in determining the pH_{opt} (19, 22). Based on

Received 4 July 2012 Accepted 13 September 2012
Published ahead of print 21 September 2012
Address correspondence to Dong-Woo Lee, leehicam@knu.ac.kr.
Sang-Jae Lee and Sang Jun Lee contributed equally to this article.
Supplemental material for this article may be found at http://aem.asm.org/.

doi:10.1128/AEM.02114-12

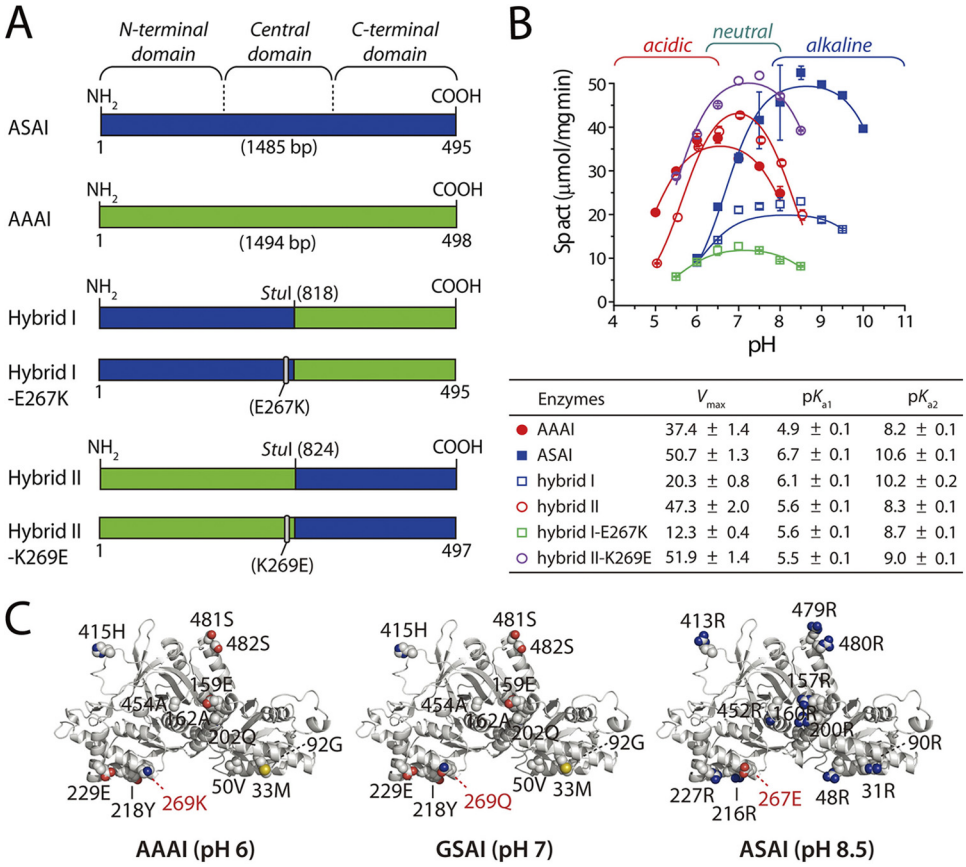

FIG 1 Schematic diagrams of the wild-type AIs and their chimeras. (A) Primary structures of the wild-type AIs and chimeras (see the supplemental material). The blue bar represents the *araA* gene encoding *Alicyclobacillus* sp. TP7 AI (ASAI), and the green bar indicates the *araA* gene encoding *A. acidocaldarius* AI (AAAI). (B) pH dependence of the wild-type AIs and chimeras based on their catalytic activity. The V_{max} data were plotted as a function of pH and fitted to a bell-shaped activity profile from the equation $V_{max} = (V_{max})_m \times [1/(1 + 10^{-pH}/10^{-pKa1} + 10^{-pKa2}/10^{-pH})]$, where apparent pK_a values corresponding to the acidic (pK_{a1}) and basic (pK_{a2}) limbs were determined by nonlinear least-squares fitting. Sp act, specific activity. (C) The hypothetical three-dimensional (3D) structures of AAAI, GSAI, and ASAI based on the crystal structure of ECAI (Protein Data Bank [PDB] 2AJT) were generated with the SWISS-MODEL program, and the locations of distinct charged amino acids on their surface and side chains of amino acid residues are depicted in spheres. Carbon, nitrogen, oxygen, and sulfur atoms are indicated in white, blue, red, and yellow, respectively. GSAI, *G. stearothermophilus* AI.

these data, a comparison of the sequence of the alkaline ASAI with the sequences of acidic AAAI and neutral *Geobacillus stearothermophilus* AI (GSAI) revealed two remarkable features (see Fig. S2 in the supplemental material). First, ASAI contains E267, which corresponds to K269 in AAAI as the "A residue," defined as ionizable groups that are directly involved in catalysis by amino acids with different charge or pK values (19, 26, 28). This was further confirmed using the hybrids I-E267K and II-K269E (see below). Second, ASAI was richer in R, which has the highest pK_a value, than AAAI (see Table S2 in the supplemental material). To investigate these characteristics, we generated several chimeric enzymes (see the supplemental material). In these chimeras, the N- or C-terminal regions were exchanged with the corresponding regions of their acidic or alkaline counterparts (Fig. 1A). The four chimeras were expressed as catalytically active and soluble forms in *E. coli* BL21(DE3) and purified for detailed characterization.

pH dependence of the activity and stability of hybrid AIs. For comparison with the wild-type AIs, analogous studies of the pH dependence of activity and stability were conducted with four hybrids. Hybrid I showed a pH_{opt} range of 7.5 to 8.0, whereas hybrid II exhibited a pH_{opt} range of 6.5 to 7.0, and its pH activity profile was similar to that of AAAI (Fig. 1B). Notably, the optimal temperatures (T_{opt}) of all hybrid AIs ranged from 60 to 70°C, indicating that they had retained their thermophilic properties (Table 1). To investigate whether the A residue can alter the pH_{opt} of hybrids I and II, the effect of pH on activity was studied using hybrids I-E267K and II-K269E. Hybrid I-E267K showed a pH_{opt} range of 7.0 to 7.5, although its pH stability was maximal at pH 9. Likewise, although the hybrid II-K269E pH_{opt} of 6.5 to 7.0 was altered to 7.5, its pH stability was maximal at pH 7.

To examine the pH dependence of protein stability in detail, the GdnHCl-induced unfolding of hybrid AIs at 25°C was investigated by monitoring the circular dichroism (CD) signals (see Fig. S3 in the supplemental material). Unfolding of the AIs involves highly cooperative transitions between the native and unfolded states, with no detectable intermediates. The midpoint concentration (C_m) of the unfolding transition for ASAI at pH 9 (2.4 M) was higher than that of AAAI (1.6 M). On the other hand, the C_m value for ASAI at pH 5 (0.8 M) was lower than that of AAAI (1.2 M). Hybrid I and hybrid II showed similar C_m values that were higher at pH 9 than at pH 7. The transitions of hybrids I and II at pH 5 were 0.5 M for hybrid I and 1.0 M for hybrid II, whereas their C_m

TABLE 1 pH dependence of the activity and stability of wild-type and hybrid AIs

Enzyme	$Temp_{React}$ (°C)[a]	pH_{opt}	pH	$pH_{1/2}$ (h)[b]
ASAI	70	8.5–9.0	5	6.9 ± 0.3
			7	201.0 ± 13.4
			9	334.0 ± 37.1
AAAI	65	6.0–6.5	5	14.0 ± 1.1
			7	90.0 ± 8.2
			9	64.6 ± 4.2
Hybrid I	65	7.5–8.0	5	10.5 ± 0.0
			7	86.0 ± 2.5
			9	94.1 ± 5.9
Hybrid II	60	6.5–7.0	5	14.8 ± 1.1
			7	59.0 ± 5.8
			9	43.0 ± 1.8
Hybrid I-E267K	65	7.0–7.5	5	8.5 ± 0.5
			7	71.7 ± 3.4
			9	97.1 ± 6.3
Hybrid II-K269E	60	7.5	5	14.8 ± 1.8
			7	88.5 ± 5.2
			9	70.0 ± 6.5

[a] $Temp_{React}$, reaction temperature.
[b] The $pH_{1/2}$ is the half-life ($t_{1/2}$) of AI activity at various pH values.

TABLE 2 pH stability of the wild-type AIs and their single-amino-acid mutants

Enzyme	$Temp_{React}$ (°C)[a]	pH_{opt}	pH	$pH_{1/2}$ (h)[b]
ASAI	70	8.5	5	6.9 ± 0.3
			7	201.0 ± 13.4
			9	334.0 ± 37.1
AAAI	65	6.0–6.5	5	14 ± 1.1
			7	90.0 ± 8.2
			9	64.6 ± 4.2
ASAI-R31E	70	6.0–8.0	5	10.1 ± 0.2
			7	125.2 ± 10.4
			9	250.9 ± 20.9
AAAI-M33R	70	7.0–8.0	5	9.1 ± 0.3
			7	124.1 ± 10.3
			9	142.0 ± 20.3
ASAI-R48E	70	6.0–8.0	5	8.9 ± 0.3
			7	192.9 ± 12.4
			9	273.7 ± 24.9
AAAI-V50R	65	7.0–8.0	5	7.8 ± 0.3
			7	158.4 ± 8.3
			9	231.6 ± 17.8
ASAI-R200E	65	6.0–8.0	5	9.8 ± 0.1
			7	100.3 ± 10.0
			9	250.9 ± 20.9
AAAI-Q202R	70	7.0–8.0	5	11.8 ± 0.2
			7	100.3 ± 3.3
			9	83.2 ± 4.6
ASAI-R216E	70	7.0–7.5	5	8.6 ± 0.3
			7	200.7 ± 13.4
			9	301.0 ± 30.1
AAAI-Y218R	70	7.0–7.5	5	10.4 ± 0.1
			7	124.6 ± 5.2
			9	102.8 ± 10.6

[a] $Temp_{React}$, reaction temperature.
[b] The $pH_{1/2}$ is the half-life ($t_{1/2}$) of AI activity at various pH values.

values at pH 9 were 1.9 M and 1.6 M, respectively. These pH stability patterns coincided with those derived from the wild-type AIs, indicating that the pH stability of AI is more dependent on the N-terminal domain. Therefore, these data demonstrate that the pH_{opt} for activity and stability of AI can be altered independently.

Characterization of AI single mutants. Based on the idea that the highly conserved residues may not be responsible for the pH dependence of AIs, the amino acid sequences were aligned to identify residues in acidic and alkaline AIs not present in neutral AIs (see Fig. S2 in the supplemental material). The roles of those residues in the pH dependence of AI were then investigated. Amino acids were selected based on the following criteria: (i) titratable charged amino acids were considered; (ii) amino acids that were also found in neutrophilic AIs were excluded; (iii) amino acids in ASAI that had charge properties opposite those of corresponding residues in AAAI were included; and (iv) amino acids in the N-terminal domain of AIs were considered. Based on the above criteria, 12 R residues in ASAI were selected (Fig. 1C) and replaced with the corresponding residues from AAAI and vice versa (Table 2). Remarkably, ASAI mutants had the pH_{opt} of stability shifted downward from basic to acidic pH, whereas the pH_{opt} values for the stability of AAAI mutants were shifted upward from acidic to basic pH. Nevertheless, all single mutants showed T_{opt} values similar to those of the wild-type enzymes, indicating that substitution in these residues affected neither the T_{opt} nor the pH_{opt} for activity. Therefore, these data strongly suggest that these R residues in the N-terminal domain of ASAI appear to be responsible for the stability at alkaline pH.

Overall, these empirical data determined with AIs were consistent with Alexov's numerical calculations (1) indicating that the pH_{opt} of activity is not correlated with the pH_{opt} of stability (11). Therefore, this report suggests that such region-specific charged amino acids are likely to have evolved to adapt the stability of enzymes at a specific pH in a manner independent of catalytic activity. Further, altering the charged state of amino acids near catalytic sites (9, 19, 23, 28, 31) and the net charge of a region of the protein might be an efficient way to engineer the pH dependence of the activity and stability of enzymes (1, 24, 27, 28).

Nucleotide sequence accession number. The 16S rRNA gene sequence of isolate TP7 was submitted to GenBank under accession number JX218020.

ACKNOWLEDGMENTS

This work was supported by grant 311042-05-1-HD120 (AGC0891111) from the Korea Institute of Planning & Evaluation for Technology (iPET) funded by the Ministry for Food, Agriculture, Forestry and Fisheries and by a grant from the Next-Generation BioGreen 21 Program (SSAC-PJ008170), Rural Development Administration, South Korea.

REFERENCES

1. **Alexov E.** 2004. Numerical calculations of the pH of maximal protein stability. The effect of the sequence composition and three-dimensional structure. Eur. J. Biochem. **271**:173–185.
2. **Anderson DE, Becktel WJ, Dahlquist FW.** 1990. pH-induced denaturation of proteins: a single salt bridge contributes 3–5 kcal/mol to the free energy of folding of T4 lysozyme. Biochemistry **29**:2403–2408.
3. **Boer H, Koivula A.** 2003. The relationship between thermal stability and pH optimum studied with wild-type and mutant *Trichoderma reesei* cellobiohydrolase Cel7A. Eur. J. Biochem. **270**:841–848.
4. **Brett CL, Donowitz M, Rao R.** 2006. Does the proteome encode organellar pH? FEBS Lett. **580**:717–719.
5. **Buonocore V, Caporale C, De Rosa M, Gambacorta A.** 1976. Stable,

inducible thermoacidophilic alpha-amylase from *Bacillus acidocaldarius*. J. Bacteriol. **128**:515–521.
6. **Chan P, Lovric J, Warwicker J.** 2006. Subcellular pH and predicted pH-dependent features of proteins. Proteomics **6**:3494–3501.
7. **Chen Y, et al.** 2011. Complete genome sequence of *Alicyclobacillus acidocaldarius* strain Tc-4-1. J. Bacteriol. **193**:5602–5603.
8. **Chouayekh H, et al.** 2007. Characterization of an L-arabinose isomerase from the *Lactobacillus plantarum* NC8 strain showing pronounced stability at acidic pH. FEMS Microbiol. Lett. **277**:260–267.
9. **Collyer CA, Henrick K, Blow DM.** 1990. Mechanism for aldose-ketose interconversion by D-xylose isomerase involving ring opening followed by a 1,2-hydride shift. J. Mol. Biol. **212**:211–235.
10. **Dische Z, Borenfreund E.** 1951. A new spectrophotometric method for the detection and determination of keto sugars and trioses. J. Biol. Chem. **192**:583–587.
11. **Garcia-Moreno B.** 2009. Adaptations of proteins to cellular and subcellular pH. J. Biol. **8**:98. doi:10.1186/jbiol199.
12. **Honda H, Kudo T, Horikoshi K.** 1985. Molecular cloning and expression of the xylanase gene of alkalophilic *Bacillus* sp. strain C-125 in *Escherichia coli*. J. Bacteriol. **161**:784–785.
13. **Hong YH, et al.** 2007. Production of D-tagatose at high temperatures using immobilized *Escherichia coli* cells expressing L-arabinose isomerase from *Thermotoga neapolitana*. Biotechnol. Lett. **29**:569–574.
14. **Hong YH, Lee DW, Pyun YR, Lee SH.** 2011. Creation of metal-independent hyperthermophilic L-arabinose isomerase by homologous recombination. J. Agric. Food Chem. **59**:12939–12947.
15. **Jørgensen F, Hansen OC, Stougaard P.** 2004. Enzymatic conversion of D-galactose to D-tagatose: heterologous expression and characterisation of a thermostable L-arabinose isomerase from *Thermoanaerobacter mathranii*. Appl. Microbiol. Biotechnol. **64**:816–822.
16. **Kim BC, Grote R, Lee DW, Antranikian G, Pyun YR.** 2001. *Thermoanaerobacter yonseiensis* sp. nov., a novel extremely thermophilic, xylose-utilizing bacterium that grows at up to 85 degrees C. Int. J. Syst. Evol. Microbiol. **51**:1539–1548.
17. **Lee DW, et al.** 2005. Distinct metal dependence for catalytic and structural functions in the L-arabinose isomerases from the mesophilic *Bacillus halodurans* and the thermophilic *Geobacillus stearothermophilus*. Arch. Biochem. Biophys. **434**:333–343.
18. **Lee DW, et al.** 2004. Characterization of a thermostable L-arabinose (D-galactose) isomerase from the hyperthermophilic eubacterium *Thermotoga maritima*. Appl. Environ. Microbiol. **70**:1397–1404.
19. **Lee SJ, et al.** 2005. Characterization of a thermoacidophilic L-arabinose isomerase from *Alicyclobacillus acidocaldarius*: role of Lys-269 in pH optimum. Appl. Environ. Microbiol. **71**:7888–7896.
20. **Manjasetty BA, Chance MR.** 2006. Crystal structure of *Escherichia coli* L-arabinose isomerase (ECAI), the putative target of biological tagatose production. J. Mol. Biol. **360**:297–309.
21. **Mavromatis K, et al.** 2010. Complete genome sequence of *Alicyclobacillus acidocaldarius* type strain (104-IA). Stand. Genomic Sci. **2**:9–18.
22. **Rhimi M, et al.** 2009. Rational design of *Bacillus stearothermophilus* US100 L-arabinose isomerase: potential applications for D-tagatose production. Biochimie **91**:650–653.
23. **Rose IA, O'Connell EL, Mortlock RP.** 1969. Stereochemical evidence for a cis-enediol intermediate in Mn-dependent aldose isomerases. Biochim. Biophys. Acta **178**:376–379.
24. **Schäfer K, et al.** 2004. X-ray structures of the maltose-maltodextrin-binding protein of the thermoacidophilic bacterium *Alicyclobacillus acidocaldarius* provide insight into acid stability of proteins. J. Mol. Biol. **335**:261–274.
25. **Stutzenberger FJ.** 1987. Inducible thermoalkalophilic polygalacturonate lyase from *Thermomonospora fusca*. J. Bacteriol. **169**:2774–2780.
26. **Tanner KG, et al.** 1999. Catalytic mechanism and function of invariant glutamic acid 173 from the histone acetyltransferase GCN5 transcriptional coactivator. J. Biol. Chem. **274**:18157–18160.
27. **Tollinger M, Crowhurst KA, Kay LE, Forman-Kay JD.** 2003. Site-specific contributions to the pH dependence of protein stability. Proc. Natl. Acad. Sci. U. S. A. **100**:4545–4550.
28. **Tomschy A, et al.** 2002. Engineering of phytase for improved activity at low pH. Appl. Environ. Microbiol. **68**:1907–1913.
29. **Warshel A.** 1981. Calculations of enzymatic reactions: calculations of pK_a, proton transfer reactions, and general acid catalysis reactions in enzymes. Biochemistry **20**:3167–3177.
30. **Weisburg WG, Barns SM, Pelletier DA, Lane DJ.** 1991. 16S ribosomal DNA amplification for phylogenetic study. J. Bacteriol. **173**:697–703.
31. **Yun YS, et al.** 2003. Origin of the different pH activity profile in two homologous ketosteroid isomerases. J. Biol. Chem. **278**:28229–28236.